Methane and Propane Total Oxidation on Catalysts from FeLDH Precursors

ADRIANA URDA[1], IONEL POPESCU[1], IOAN-CEZAR MARCU[1*], GABRIELA CARJA[2], NICOLAE APOSTOLESCU[2], IOAN SANDULESCU[1]

[1] University of Bucharest, Faculty of Chemistry, Department of Chemical Technology and Catalysis, 4-12 Regina Elisabeta Bd., 030018, Bucharest, Romania

[2] "Al. I. Cuza" Technical University Iaşi, 59 D. Mangeron Bd., 700050, Iasi, Romania

Total catalytic oxidation of methane and propane was performed on mixed oxides obtained from a Fe/FeLDH precursor calcined at different temperatures: 550°, 650° and 750°C. The textural properties of the samples, determined by N_2 adsorption-desorption at -196°C, depended on the calcination temperature. The specific surface area (S_{BET}) and the pore volume (V_p) decreased when the calcination temperature increased. These changes are possibly due to the sintering phenomena in the solid accompanied by micropores closure. The catalytic properties were not influenced by the calcination temperature, the activity being determined by the nature of hydrocarbon that was subjected to the total oxidation reaction, and by the reaction temperature. The conversions were functions of hydrocarbon concentration in the reaction mixture and increased with reaction temperature.

Keywords: catalytic oxidation, textural properties, calcination temperature, pore volume, catalytic properties

Nowadays, there have been continuing efforts to develop new and improved catalytic systems for removing toxic environmental pollutants. CO removal from flue gases is a well-known process [1]; for other volatile organic compounds (VOCs) research is on-going in order to find efficient, stable and non-expensive catalytic systems [2-5]. Recently reported results showed that some cost effective and promising catalytic systems for the total oxidation of methane and propane are based on iron containing oxides [6-9]. The nature of the active sites, but also the catalyst textural and surface properties are important factors determining the catalyst performance; the specific characteristics of the catalyst nanoparticles and/or their agglomerations, their shape, size and organization pattern that give rise to tailored nanoporous properties and high surface areas may open new possibilities for designing better catalysts [10, 11].

Represented by the general formula $[M^{II}_{1-x}M^{III}_{x}(OH)_2]^{x+}[A^{m-}_{x/m}\cdot nH_2O]^{x-}$, layered double hydroxides anionic clays (LDHs) are built up of edge-sharing metal octahedral sheets, where, by comparison to brucite $M(OH)_2$, part of M^{II} is replaced by M^{III} metal cations; the excess of the positive charge is counterbalanced by exchangeable anions, A^{m-}, located, as well as water molecules, in the interlayer space [12]. The large variety of compositions that can be developed by changing the nature of the divalent and trivalent cations (M^{II}, M^{III}), the interlayer anions (A^{m-}) and the stoichiometric coefficient (x) give rise to a large diversity of layered anionic clay – like structures [13]. The thermal decomposition of hydrotalcite-like materials around 500°C produces stable homogeneous and highly dispersed mixed metal oxides with a high surface area and displaying specific acid - base / redox and textural properties, with well-known applications as catalysts [13-18].

Based on this information, we present original results concerning the use of iron oxides supported on nanostructured formulations based on iron substituted hydrotalcite-like anionic clays, as catalyst precursors for the total oxidation of methane and propane. We report the influence of the catalyst textural properties on the catalytic performances in the total oxidation of methane and propane.

Experimental part

Catalysts preparation

The iron containing LDH precursor (denoted as FeLDH) was synthesized by the co-precipitation method [19] from metal salts aqueous solutions ($Mg(NO_3)_2\cdot 6H_2O$, $FeSO_4\cdot 7H_2O$ and $Al(NO_3)_3\cdot 9H_2O$ – molar ratio = 2/0.5/0.5). The precipitating agent aqueous solution ($NaOH/Na_2CO_3$, 1 M) was added at 37°C, under constant nitrogen flow by stirring at constant pH of 8.9 ± 0.2. The precipitate was aged, separated by centrifugation, washed with warm double deionized water until sodium free, dried under vacuum overnight and then calcined in air at 450°C for 7 h with a heating rate of 8°C min^{-1}.

The iron oxide–LDH ensemble (denoted as Fe/FeLDH), used as catalyst precursor, was prepared [19] by adding the calcined FeLDH clay powder to a $FeSO_4$ aqueous solution (1 M), under stirring and nitrogen atmosphere (the volume of the $FeSO_4$ solution was calculated so that the SO_4^{2-} concentration has exceeded two times the exchange capacity of the clay), then aged at 65°C.

The Fe/FeLDH sample was then calcined at three different final temperatures: 550, 650 and 750°C (heating rate 10°C min^{-1}, the final temperature being maintained for 10 h).

Catalysts characterization

Elemental analyses were performed by ICP emission spectroscopy, with a SPECTROFLAME-ICP spectrometer, using solutions prepared by dissolving the samples in dilute H_2SO_4.

X-ray powder diffraction patterns were recorded on a DRON-2 diffractometer equipped with a Cu Kα source (λ = 1.54 Å). They were recorded over the 10–70° angular range with a 0.02° step and an acquisition time of 1 s per point.

* *email: ioancezar_marcu@yahoo.com; Tel.: 0727634144*

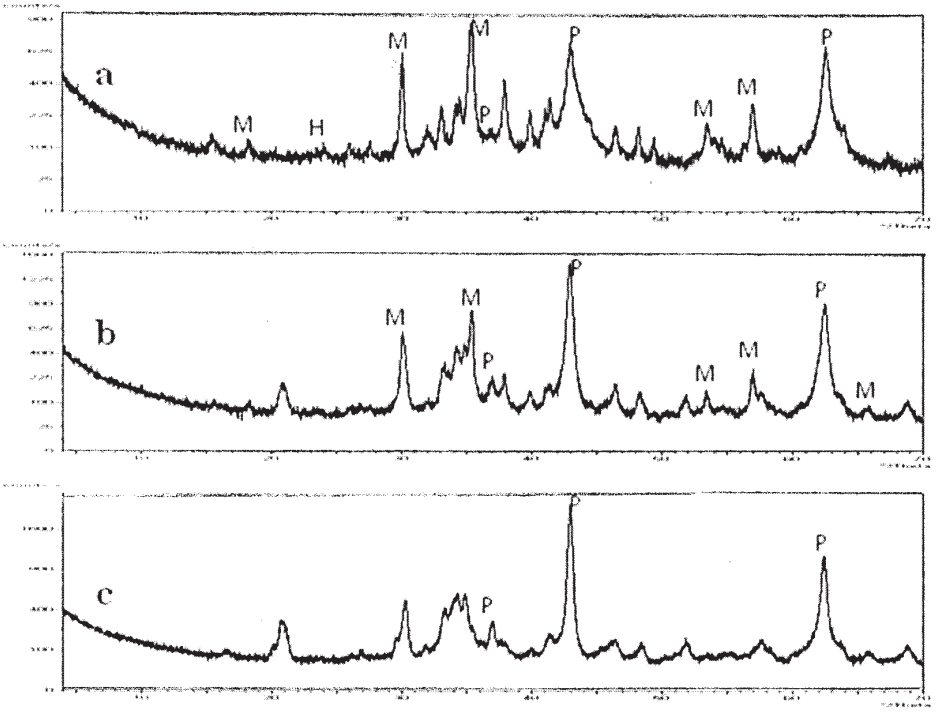

Fig. 1. XRD patterns of the calcined samples: (a) 550°C; (b) 650°C; (c) 750°C; P – periclas (MgO), M – magnetite (Fe_3O_4), H – hematite (Fe_2O_3)

N_2 adsorption isotherms were measured at -196°C on a Micromeritics ASAP 202 V3.00 H automated gas adsorption system. Prior to the measurements, the samples were heated for 10 h under vacuum at 200°C (heating rate 10°C min^{-1}). The BET specific surface area (S_{BET}) was calculated by using the standard Brunauer, Emmet and Teller method on the basis of the adsorption data. The pore size distributions were calculated from the desorption branches of the isotherms using the Barrett-Joyner-Halenda method.

IR spectra were recorded on a Shimadzu FTIR spectrometer under the following experimental conditions: 200 scans in the mid-IR range (500-4000 cm^{-1}) using KBr (ratio 5 / 95 wt %) pellets, and a resolution of 4.0 cm^{-1}.

TEM analysis was performed on a Hitachi instrument operating at 200 kV. The samples were prepared by dispersing them in ethanol.

Catalytic tests

The total oxidation reactions were carried out in a fixed bed quartz tube down-flow reactor operated at atmospheric pressure. The internal diameter of the reactor tube was 18 mm, and the catalyst was supported by quartz wool. The axial temperature profile was measured using an electronic thermometer placed in a thermowell centered in the catalyst bed. Quartz chips were used to fill the dead volumes before and after the catalyst bed, in order to minimize potential gas-phase reactions. For the methane combustion, the reaction mixture consisted of 1 and 5%(vol.) methane in air. For propane total oxidation reactions, the propane concentration was calculated in order to have similar carbon content to the methane experiments – 0.33 and 1.67% (vol.), respectively. Flow rates were controlled by fine needle valves and were measured by capillary flow-meters. Catalytic tests were performed at total volume hourly space velocity (VHSV) of 16000h^{-1}, in the temperature range 380 – 750°C. The highest reaction temperature on each sample was equal to the calcination temperature.

In a typical reaction run, the reactor containing 1 cm^3 of catalyst was heated to the desired temperature in the flow of reactants. The system was allowed to stabilize for about 1 h at the reaction temperature before the first product analysis was made. Each run was carried out over a period of at least 1 hour, until two consecutive analyses were identical. A Thermo Finnigan (CE Instruments) gas chromatograph, equipped with a flame ionization detector (FID) and a thermal conductivity detector (TCD) was used, and the chromatographic separation was accomplished with an alumina column (FID detector) and a CTR I column (TCD detector). The conversion was calculated as the amount of raw material transformed in reaction divided by the amount that was fed to the reactor. Complete selectivity to CO_2 and H_2O was always observed.

Results and discussion

Catalysts properties

The elemental analysis, composition and textural characteristics of the LDH samples were reported elsewhere [19]. Consequently, the elemental analysis for the FeLDH sample indicated a Mg^{2+}:Fe^{3+} ratio of 1.91, with 30.4 % (mass) Fe. After the deposition of iron oxide on the surface, the Mg^{2+}:Fe^{3+} ratio decreased to 0.74, and the iron content rised to 43.7 % (mass). The XRD patterns of the obtained LDH-type samples indicated characteristic reflections of LDHs, with sharp and simetric peaks at low 2θ angles, but broad and assimetric at high 2θ angle. For the Fe/FeLDH sample the intensity of the diffraction peaks decreases in comparison with the original LDH, probably due to a lower crystallinity and different textural characteristics of the sample.

The XRD patterns of the calcined samples are shown in figure 1.

Calcination at 550°C leads to the destruction of the layered LDH network, giving rise to amourphous-like patterns, characteristic to mixed oxides with poor crystallinity, but well dispersed. As the calcination temperature increses the intensity of the peaks accentuates, indicating a higher crystallinity of the samples. As indicated in figure 1, periclas, magnetite and hematite peaks were identified.

The FTIR analysis gives information about the nature of the anions from the clay interlayers. The FTIR patterns, shown in figure 2, reveal some similarity for the FeLDH and the Fe/FeLDH layered structures. The broad absorption peaks in the region 2800-3600 cm^{-1} and 1560 cm^{-1} are

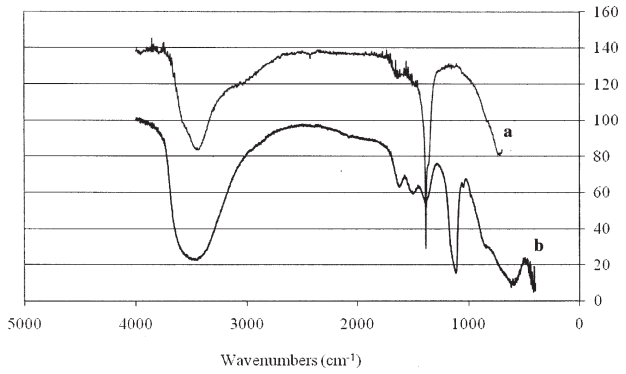

Fig. 2. FTIR patterns for the FeLDH (a) and Fe/FeLDH (b) samples

attributed to the O-H symmetric stretching mode and bending modes in the metal hydroxide layers or interlayer water molecules. The band corresponding to the bending mode δ_{OH} appears between 1644-1648 cm^{-1} and may be assigned to the adsorbed interlayer water. An intense absorption band between 1370-1383 cm^{-1} is attributed to the ν_3 vibration mode of CO_3^{2-} [20]. In the same range, the ν_3 vibration mode of the nitrate could appear if this still exists in the interlayer. For Fe/FeLDH, a new band was observed at 1122 cm^{-1} assigned as the ν_3 vibration mode of SO_4^{2-} and recognized the presence of SO_4^{2-} in the clay interlayer. In the low wavenumber region (< 1000 cm^{-1}) the lattice vibration modes of the LDH sheets such as M-O (550, 590 and 840 cm^{-1}) and O-M-O (430 cm^{-1}) vibrations are observed.

TEM analysis offers a deeper look on the morphologic features of the new catalytic material. For the Fe/FeLD structure, the TEM picture (fig. 3) reveals [21] that nanoparticles with the average diameter of 27 nm exist on the larger nanoparticles of iron substituted clay.

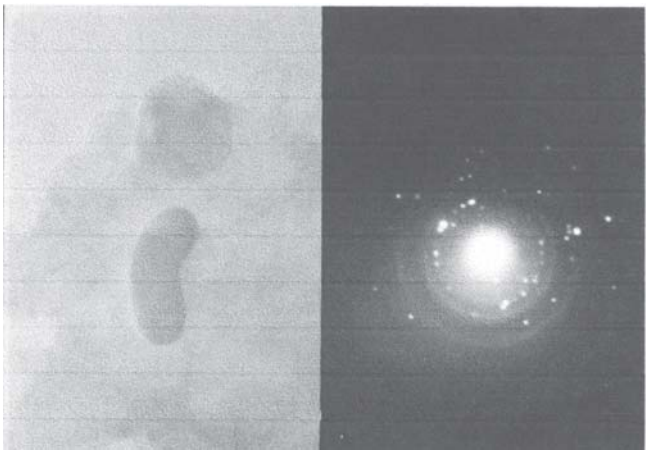

Figure 3. The TEM image for the Fe/FeLDH sample

N_2 adsorption at -196°C was used to get information about the textural characteristics and the specific surface area of the samples. Results for the calcined samples are shown in table 1.

The characteristic isotherms (presented in figure 4 for the sample calcined at 550°C) correspond to a type IV in the IUPAC classification, with a type H_1 hysteresis for the calcined samples, indicative of a narrow range of uniform mesopores [22]. The calculated BET surface area (table 1) decreases with increasing calcination temperature, probably due to sintering phenomena in the mixed oxides. Pore volumes strongly diminish as the calcination temperature rises, in correlation with the specific surface area values.

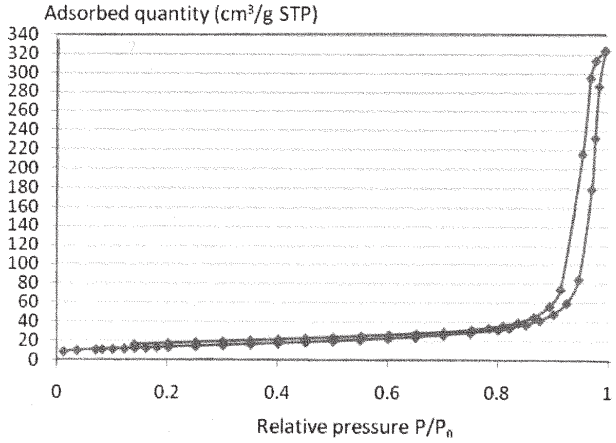

Fig. 4. N_2 adsorption-desorption isotherm of the mixed oxide sample calcined at 550°C

Catalytic tests

The calcined samples were tested in the catalytic combustion of methane and propane.

The results obtained in the catalytic tests using 5 % methane in air are presented in figure 5. As methane is difficult to be activated, high temperatures are needed for its combustion. Consequently, conversion values on the samples calcined at 550 and at 650°C are low, and the highest conversion value (71.5 %) could be reached on the sample calcined at 750°C. As the three plots actually overlap, it is obvious that all the samples show a similar catalytic behaviour, and there are no influences of the calcination temperature on the catalytic activity in the temperature range 550 – 750°C. This is in line with XRD patterns of the three calcined samples, showing only increased crystallinity with higher calcination temperature. Specific surface area and pore volume differences seem to be of lesser importance for these catalysts.

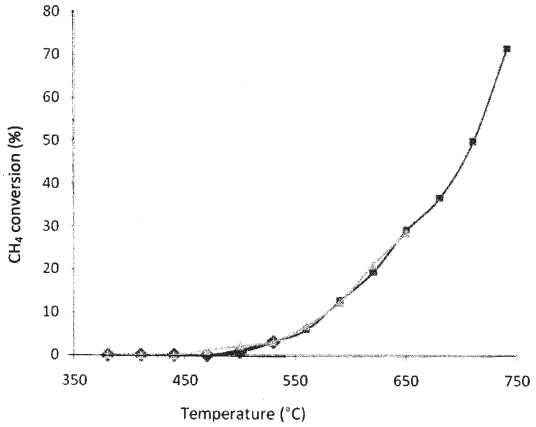

Fig. 5. Effect of the reaction temperature on the conversion of methane in the catalytic combustion reaction; (♦) sample calcined at 550°C; (▲) sample calcined at 650°C; (■) sample calcined at 750°C; total VHSV = 16.000 h^{-1}, methane concentration: 5 % in air

Calcination temperature (°C)	S_{sp}, BET ($m^2\ g^{-1}$)	Pore volume ($cm^3\ g^{-1}$)
550	49	0.50
650	27	0.31
750	18	0.14

Table 1
SPECIFIC SURFACE AREA (S_{sp}, BET) AND PORE VOLUME FOR THE LDH AND MIXED OXIDES SAMPLES

Figure 6 presents results of the combustion reaction with 1% methane for the catalysts calcined at 550 and 750°C. In comparison with the plots from figure 5, conversion values are higher, as expected, reaching 100% at 700°C for the sample calcined at 750°C.

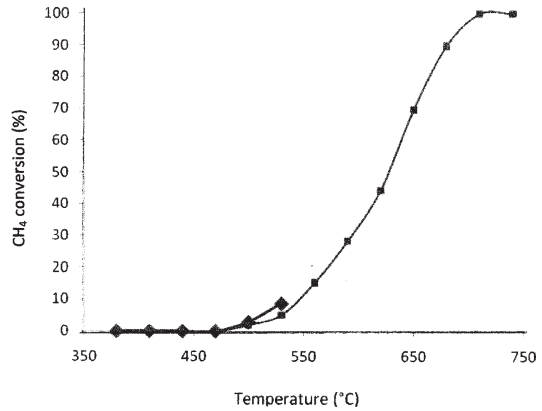

Fig. 6. Effect of the reaction temperature on the conversion of methane in the catalytic combustion reaction; (♦) sample calcined at 550°C; (■) sample calcined at 750°C; total VHSV = 16.000 h^{-1}, methane concentration: 1 % in air.

In order to investigate the influence of the alkane reactivity, similar combustion tests using propane were performed. The results obtained at 1.67% C_3H_8 (the same carbon content as in the reaction mixture with 5% methane) are presented in figure 7. Because propane is easier to activate, conversion values are higher than those with methane, and total conversion was attained at 700°C. Again, the behaviour of the three samples was similar, showing no notable differences at the same reaction temperature.

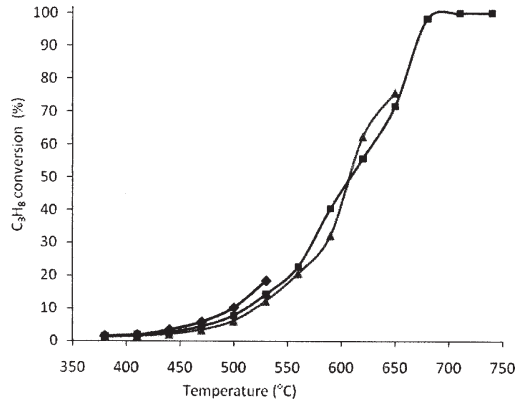

Fig. 7. Effect of the reaction temperature on the conversion of propane in the catalytic combustion reaction; (♦) sample calcined at 550°C; (▲) sample calcined at 650°C; (■) sample calcined at 750°C; total VHSV = 16.000 h^{-1}, propane concentration: 1.67 % in air

Catalytic tests were also performed using 0.33 % C_3H_8 (the same carbon content as in the reaction mixture with 1 % methane), and the results are shown in figure 8 for the catalyst calcined at 750°C, in comparison with the results obtained with 1.67% propane. For the smaller concentration, total conversion was reached at 600°C, 100° lower than in the previous case. Moreover, the same temperature difference can be observed for the T_{50} values (T_{50} – the temperature necessary for a 50% conversion), both in the case of methane and propane reactions. Therefore, alkane concentration is an important factor for the total combustion temperature: the smaller the concentration, the lower the temperature that is necessary for total oxidation.

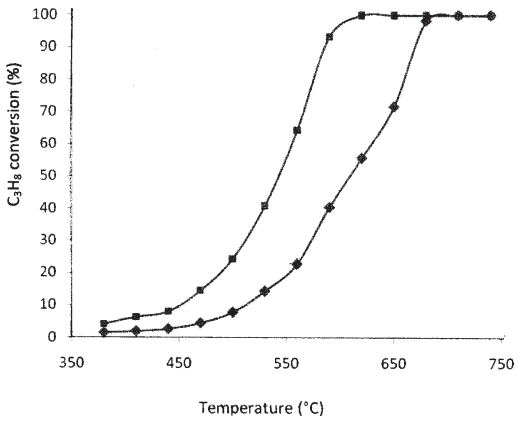

Fig. 8. Effect of the reaction temperature on the conversion of propane (0.33 %, ■ and 1.67 %, ♦) in the catalytic combustion reaction; total VHSV = 16.000 h^{-1}

Conclusions

Three catalyst samples, obtained from Fe/FeLDH clays by calcination at 550, 650 and 750°C, were tested in the catalytic combustion of methane and propane. By calcining at temperatures higher than 500°C, LDH clays were transformed into well-dispersed mixed oxides, their crystallinity increasing with temperature. Specific surface areas, as well as pore volumes, decreased at higher calcination temperature, probably due to sintering phenomena in the mixed oxides. However, their catalytic behaviour was similar in the combustion reactions, both in the case of methane and propane reactions. The temperature needed for total conversion depends on the nature of the hydrocarbon and on its concentration in the reaction mixture: propane is more easily destroyed by combustion than methane, and the smaller the concentration, the lower the temperature for 100 % conversion.

Acknowledgements: This research was supported by the PNCDI II contract NATOEPA 71-020/2007.

References

1.HUTCHINGS, G.J., SCURRELL, M.S., CATTECH, **7**, nr. 3, 2003, p. 90
2.GENNEQUIN, C., COUSIN, R., LAMONIER, J.-F., SIFFERT, S., ABOUKAIS, A., Catalysis Communication **9**, 2008, p. 1639
3.OLIVEIRA, L.C.A., LAGO, R.M., FABRIS, J.D., SAPAG, K., Applied Clay Science, **39**, nr. 3-4, 2008, p. 218
4.GEORGESCU, V., BOMBOS, D., SCURTU, R., SPASSOVA, I., MEHANDJIEV, D., DUMITRACHE, L. D., Rev. Chim. (Bucuresti), **59**, no. 2, 2008, p. 243
5.CHIOARU, L. C., JITARU, I., BICHER, M., MATEI. V., MIHAI, O., Rev. Chim. (Bucuresti), **60**, no. 3, 2009, p. 283
6.SCIRE, S., MINICO, S., CRISAFULLI, C., GALVAGNO, S., Catalysis Communications, **2**, 2001, p. 229
7.YIN, F., JI, S., CHEN, B., ZHAO, L., LIU, H., LI, C., Applied Catalysis B: Environmental, **66**, 2006, p. 265
8.MORALES, M.R., BARBERO, B.P., CADUS, L.E., Applied Catalysis B: Environmental, **74**, 2007, p. 1
9.URDA, A., HERRAIZ, A., REDEY, A., MARCU I.-C., Catalysis Communications, **10**, 2009, p. 1651
10.CARJA, G., OBATA, H., KAMESHIMA Y., OKADA K., Microporous and Mesoporous Materials, **98**, nr. 1-3, 2007, p. 150
11.HADNADJEV, M., VULIC, T., MARINKOVIK-NEDUCIN, R., SUCHORSKI, Y., WEISS, H., Applied Surface Science, **254**, 2008, p. 4297
12.VACCARI A., Catalysis Today, **41**, 1998, p. 53-71
13.KOVANDA F., ROJKA T., DOBESOVA, J., MACHOVIC, V., BEZDICKA, P., OBALOVA, L., JIRATOVA, K., GRYGAR, T., Journal of Solid State Chemistry, **179**, 2006, p. 812

14.SELS, B., DE VOS, D.E., JACOBS, P.A., Catalysis Reviews: Science and Engineering, **43**, nr. 4, 2001, p. 443
15.DULA, R., JANIK, R., MACHEJ, T., STOCH, J., GRABOWSKI, R., SERWICKA, E.M., Catalysis Today, **119**, 2007, 327
16.CENTI, G., PERATHONER, S., Microporous and Mesoporous Materials, **107**, 2008, p. 3
17.KSONTINI, N., NAJJAR, W., GHORBEL, A., Journal of Physics and Chemistry of Solids, **69**, nr. 5-6, 2008, p. 1112
18.TANASOI, S., TANCHOUX, N., URDA, A., TICHIT, D., SANDULESCU, I., FAJULA, F., MARCU, I.-C., Applied Catalysis A: General, **363**, 2009, p. 135
19. CARJA, G., KAMESHIMA, Y, KIYOSHI, O., Microporous and Mesoporous Materials, **115**, nr. 9, 2008, p. 541
20. PEREZ RAMIREZ, J., MUL, G., KAPTEJIN, F., MOULIJN, J.A., J. Mater. Chem., **11**, nr. 3, 2001, p. 821
21.CARJA, G., NAKAMURA, R., NIIYAMA, H., Microporous and Mesoporous Materials, **83**, nr. 1-3, 2005, p. 94
22. NEIMARK A.V., SING, K.S.W., THOMMES M., Handbook of Heterogeneous Catalysis, 2nd Edition, **2**, Wiley-VCH Verlag GmbH & Co, KGaA, Eds G. Ertl, H. Knozinger, F. Schuth, J. Weitkamp, Weinheim, 2008, p.723

Manuscript received: 1.07.2009